JOURNAL OF BACTERIOLOGY, Apr. 2008, p. 2822–2830 Vol. 190, No. 8
0021-9193/08/$08.00+0 doi:10.1128/JB.01379-07

Transcriptome Analysis of a Phenol-Producing *Pseudomonas putida* S12 Construct: Genetic and Physiological Basis for Improved Production▽†

Nick J. P. Wierckx,[1,2]* Hendrik Ballerstedt,[1,2] Jan A. M. de Bont,[2]‡ Johannes H. de Winde,[2,3] Harald J. Ruijssenaars,[1,2] and Jan Wery[2]§

TNO Quality of Life, Department of Bioconversion, Julianalaan 67, 2628 BC, Delft, The Netherlands[1]; Kluyver Centre for Genomics of Industrial Fermentation, P.O. Box 5057, 2600 GB, Delft, The Netherlands[2]; and Delft University of Technology, Department of Biotechnology, Julianalaan 67, 2628 BC, Delft, The Netherlands[3]

Received 24 August 2007/Accepted 29 October 2007

The unknown genetic basis for improved phenol production by a recombinant *Pseudomonas putida* S12 derivative bearing the *tpl* (tyrosine-phenol lyase) gene was investigated via comparative transcriptomics, nucleotide sequence analysis, and targeted gene disruption. We show upregulation of tyrosine biosynthetic genes and possibly decreased biosynthesis of tryptophan caused by a mutation in the *trpE* gene as the genetic basis for the enhanced phenol production. In addition, several genes in degradation routes connected to the tyrosine biosynthetic pathway were upregulated. This either may be a side effect that negatively affects phenol production or may point to intracellular accumulation of tyrosine or its intermediates. A number of genes identified by the transcriptome analysis were selected for targeted disruption in *P. putida* S12TPL3. Physiological and biochemical examination of *P. putida* S12TPL3 and these mutants led to the conclusion that the metabolic flux toward tyrosine in *P. putida* S12TPL3 was improved to such an extent that the heterologous tyrosine-phenol lyase enzyme had become the rate-limiting step in phenol biosynthesis.

Pseudomonas putida is a ubiquitous soil bacterium that has become increasingly important for a wide range of biotechnological applications (46). Its broad biocatalytic potential makes it highly suitable for applications such as bioremediation (8) and biocatalysis (7, 40). Of special interest are solvent-tolerant *P. putida* strains. These organisms have evolved several mechanisms to deal with toxic compounds, including modifications of the inner and outer membranes and active extrusion of a broad range of compounds through membrane-associated efflux pumps (18, 31, 32). Solvent-tolerant bacteria are especially useful for the biosynthesis of compounds that are toxic to other microorganisms (7, 39, 48). They have been used to produce different aromatic compounds, such as cinnamic acid (24), *p*-hydroxybenzoic acid (33, 43), 3-methylcatechol (35, 50), and phenol (51).

Previously, we reported the construction of a *P. putida* S12 strain which efficiently produces phenol from glucose as a demonstration case for the "green" production of a toxic, hydroxylated aromatic compound (51). This strain has since been converted into an efficient producer of other, value-added aromatics (43). Efficient phenol production was achieved by introduction of the *tpl* gene from *Pantoea agglomerans*, encoding the enzyme tyrosine-phenol lyase (TPL), followed by a combined approach of targeted genetic engineering, random mutagenesis, antimetabolite selection, and high-throughput screening. This approach resulted in strain *P. putida* S12TPL3, which was capable of converting glucose into phenol with a yield of 7% (mol/mol) (51). The optimization of phenol production was achieved mostly by random approaches. As a result, little is known about the genetic basis of the enhanced phenol production.

Transcriptome analysis has been used successfully in the past to gain comprehensive insight into complex metabolic networks (12, 27, 29) and organic solvent stress (10, 14, 34). This technique has also been successfully applied for the analysis and optimization of microbial production strains (6, 20, 25). Since the genome sequence of *P. putida* KT2440 has become available (23), this avenue of research is open for the study of *P. putida* species. Ballerstedt et al. (2) demonstrated that microarrays based on this genome sequence are suitable for the analysis of *P. putida* strain S12.

The goal of this work was to identify the cellular mechanisms that underlie the optimized phenol production and to identify possible bottlenecks for phenol production of strain S12TPL3. To this end, we performed comparative transcriptomics, complemented with nucleotide sequence analysis and disruption of key genes involved in phenol production.

MATERIALS AND METHODS

Strains and growth conditions. The bacterial strains and plasmids used in this study are listed in Table 1. *P. putida* S12 was originally isolated as a styrene-degrading bacterium (13). *P. putida* S12JNNmcs(t) is a negative control strain obtained by transforming *P. putida* S12 with the empty expression vector pJNNmcs(t) (previously known as pTn-1) (24, 51). *P. putida* S12TPL3 is a mutant optimized for phenol production (Fig. 1). *P. putida* S12TPL3c was obtained by serial cultivation of *P. putida* S12TPL3 in LB medium with 50 mg · liter^{-1} kanamycin. After five cultivations, the culture was streaked on LB agar with kanamycin. Separate colonies were inoculated on LB agar with 30 mg · liter^{-1} gentamicin. Colonies that had lost their Gm^r phenotype were considered to be cured of the pNW1C plasmid.

Culture conditions for shake flask cultivations, as well as medium composi-

* Corresponding author. Mailing address: TNO Quality of Life, P.O. Box 5057, 2600 GB, Delft, The Netherlands. Phone: 31-15-2787905. Fax: 31-15-2782355. E-mail: nick.wierckx@tno.nl.

† Supplemental material for this article may be found at http://jb.asm.org/.

‡ Present address: Royal Nedalco, Van Konijnenburgweg 100, Bergen op Zoom, 4612 PL, The Netherlands.

§ Present address: Dyadic Nederland BV, Nieuwe Kanaal 7^s, 6709 PA Wageningen, The Netherlands.

▽ Published ahead of print on 9 November 2007.

TABLE 1. Bacterial strains and plasmids used in this study

Strain or plasmid	Relevant characteristics[a]	Reference(s)
Strains		
E. coli DH5α	*supE44* Δ*lacU169* (ϕ80 *lacZΔM15*) *hsdR17 recA1 endA1 gyrA96 thi-1 relA1*	37
P. putida		
S12	Wild type	13, 47
S12JNNmcs(t)	S12 transformed with empty expression vector pJNNmcs(t); negative control	51
S12TPL3	Phenol-overproducing mutant of S12	51
S12TPL3c	S12TPL3 without vector pNW1C	This study
S12TPL3r	S12TPL3c retransformed with vector pNW1C	This study
STΔpobA	S12TPL3 *pobA*::*tetA*	This study
STΔaroP1	S12TPL3 *aroP1*::*tetA*	This study
STΔhpd	S12TPL3 *hpd*::*tetA*	This study
STΔphhA	S12TPL3 *phh*::*tetA*	This study
Plasmids		
pNW1C	Gm^r Ap^r; expression vector with *tpl* under control of the *nagR/pNagAa* promoter	51
pJQ200SK	Gm^r; gene replacement vector	30
pTO1	Tc^r; *tetA* donor plasmid	49
pJQpobA::tetA	Tc^r Gm^r; pJQ200SK with the *pobA* gene interrupted by the *tetA* gene	43
pJQaroP1::tetA	Tc^r Gm^r; pJQ200SK with the *aroP1* gene interrupted by the *tetA* gene	This study
pJQhdp::tetA	Tc^r, Gm^r; pJQ200SK with the *hpd* gene interrupted by the *tetA* gene	This study
pJQphhA::tetA	Tc^r Gm^r; pJQ200SK with the *phhA* gene interrupted by the *tetA* gene	This study

[a] Ap^r, Gm^r, and Tc^r, ampicillin, gentamicin, and tetracycline resistance, respectively.

tions, were as described previously (51), except that 10 mM glucose was used in phenol production experiments. Chemostat cultivations were performed in 1-liter fermentors (New Brunswick Scientific) with a BioFlo 110 controller. Chemostats were inoculated with a 35-ml shake flask culture grown for approximately 8 hours in mineral salts medium (13) with 20 mM glucose supplemented with 10 mg · $liter^{-1}$ gentamicin and 0.1 mM salicylate. The chemostat cultures were fed with the same medium containing 10 mM glucose as the growth-limiting nutrient. The working volume of the culture was kept at 0.7 liter by removing culture broth via a continuously working pump. The dilution rate (D) was set at 0.05 h^{-1} for 16 h, after which it was increased to 0.2 h^{-1}. The pH was maintained at 7.0 by automatic addition of 4.0 M NaOH, and the temperature was kept at 30°C. Air was supplied with a flow of 1.0 liter · min^{-1} into the headspace. Dissolved oxygen levels were maintained at 15% air saturation by automatic adjustment of the stirring speed. Cultures were considered to be at steady state when after at least five volume changes at $D = 0.2$ h^{-1}, there was no significant change in the phenol concentration in the fermentor, the optical density at 600 nm, and the stirring speed.

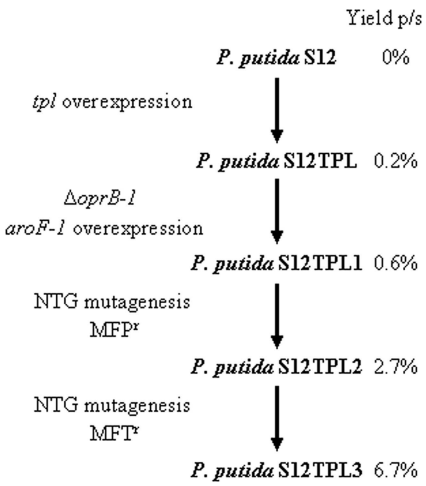

FIG. 1. Genealogy of phenol-producing mutants of *P. putida* S12. The left column shows how each successive mutant was obtained. The right column indicates the yield (mol phenol/mol glucose) attained in a typical shake flask culture (51). NTG, *N*-methyl-*N*′-nitro-*N*-nitrosoguanidine; MFP^r: resistant to 100 mg *m*-fluoro-DL-phenylalanine · $liter^{-1}$; MFT^r, resistant to 100 mg *m*-fluoro-L-tyrosine · $liter^{-1}$.

Sampling, mRNA isolation, and cDNA preparation for microarray analysis. Chemostat samples were quenched in ice-cold methanol and centrifuged, and 1 ml RNAlater (Ambion) was added to the pellet. The cells were incubated for at least 1 h at 4°C, after which RNAlater was removed and the pellet flash frozen in liquid nitrogen and stored at −80°C. Frozen cell pellets were thawed by resuspension in 100 μl Tris-EDTA buffer containing 1 mg · ml^{-1} lysozyme. Total RNA was subsequently isolated using the Qiagen RNeasy mini purification kit according to the manufacturer's instructions. DNA was removed by on-column DNase I digestion, and total RNA was concentrated using the Qiagen RNA MinElute kit. mRNA was enriched using the Ambion MICROBExpress bacterial mRNA purification kit in combination with the specialized module for *Pseudomonas* according to the manufacturer's instructions. RNA concentrations were determined using an ND-1000 Nanodrop spectrophotometer (Isogen Life Sciences), and RNA quality was verified using the Bio-Rad Experion system (Bio-Rad) in combination with the Experion RNA standard- and high-sense analysis kit. Random priming cDNA synthesis, purification, fragmentation, and labeling were performed according to the microarray manufacturer's instructions (Affymetrix).

Microarray analysis. High-density microarrays based on the genome of *P. putida* KT2440 were used (2). An additional 95 probe sets were added to this basic array, based on known sequences of *P. putida* S12 and related strains. A complete list of the features covered by these probe sets can be found in Table S1 in the supplemental material. The end-labeled cDNA fragments were hybridized to the microarray according to standard manufacturer's protocols. The chips were scanned, and the resulting .cel files were imported into Genespring GX software package version 7.2 (Agilent) using the GC RMA algorithm. After normalization, one-way analysis of variance ($P > 0.05$) was used to select genes that changed significantly between the conditions tested. Genes whose the expression level differed at least 1.8-fold between the two analyzed strains were used for further analysis.

Verification of transcriptome analysis by RT-qPCR. The mRNA levels of a subset of genes were verified by real-time quantitative PCR (RT-qPCR). Specific primers (see Table S2 in the supplemental material) were designed using Primer3 software (http://frodo.wi.mit.edu/) (length maximum, 20 bases; G/C content, 50 to 60%; T_m, 55 to 60°C). PCR primer target sequences were chosen to achieve amplicon lengths of 75 to 200 bp. To predict possible amplicon secondary structures, Mfold software (http://www.bioinfo.rpi.edu/applications/mfold/) was used. RT-qPCR was performed with a spectrofluorimetric thermal cycler (iQ Cycler

with optical module; Bio-Rad) using the iScript one-step RT-PCR kit with Sybr green (Bio-Rad) and equal amounts total RNA samples (100 ng) in 96-well plates according to the manufacturer's protocols (annealing temperature, 58°C). The RNase inhibitor SuperaseIn (Ambion) was added at a concentration of 0.5 U/μl to all RT-qPCR batches. Calibration curves relating the threshold cycle as a function of the log of the copy number of target gene were established using 10-fold serial dilutions (10 to 10^7 gene copies μl^{-1} template DNA) of *P. putida* S12 genomic DNA. All absolute quantifications were obtained using iCycler iQ real-time detection system software version 3.1 (Bio-Rad).

Nucleotide sequence analysis of key genes. A total of 15 genes involved in the biosynthesis and degradation of tyrosine and phenol were selected for sequencing from both wild-type *P. putida* S12 and phenol-producing *P. putida* S12TPL3. PCR primer pairs were designed based on the genome sequence of *P. putida* KT2440 (23) and used to amplify the specific genes from the genomes of the two strains (see Table S2 in the supplemental material). PCR fragments were purified, and their nucleotide sequences were determined with the primers used for amplification. If a mutation was observed, PCR fragments were amplified and sequenced a second time to confirm the result. The *tpl* gene was sequenced on the plasmid isolated from *P. putida* S12TPL3 (primers are listed in Table S2 in the supplemental material). Nucleotide sequence analyses were performed by MWG-Biotech AG.

Targeted gene disruption. Targeted gene disruptions were performed basically as described previously (43). Gene replacement vectors for the *hpd*, *pobA*, *phhA*, and *aroP1* genes (Table 1) were created from pJQ200SK (30) with primers listed in Table S2 in the supplemental material. These vectors were used to mutate the selected genes in *P. putida* S12TPL3c by homologous recombination. Subsequently, pNW1C was transformed into the mutants by electroporation to yield *P. putida* STΔhpd, STΔpobA, STΔphhA, and STΔaroP1 (Table 1). All DNA manipulations were performed under permit DGM/SASIG 02-118 of the Dutch government.

TPL activity assay. Cell extracts of *P. putida* S12TPL3 were produced by sonication as described previously (51) from a 100-ml shake flask culture in mineral salts medium with 20 mM glucose, 10 mg/liter gentamicin, and 0.1 mM salicylate. The conditions for the TPL activity assay were adapted from reference 19. To 1 ml of cell extract, 1.25 mM L-tyrosine and 0.1 mM pyridoxal 5′-phosphate were added. Three different concentrations of phenol (0, 0.25, and 1 mM) were added to study the effect of product inhibition. The reaction was carried out at 30°C. Samples were drawn after 0, 2, 5, 15, and 30 min, and the reaction was stopped by addition of 7.5% trichloroacetic acid. The pyruvate concentration in the samples was measured as described below. Pyruvate was measured instead of phenol because of the high background concentration of phenol already present in most samples.

Analytical methods. Cell density, phenol, glucose, gluconic acid, 2-ketogluconic acid, and ammonium concentrations were determined as described previously (51). Pyruvate concentrations were determined by high-pressure liquid chromatography (HPLC) (Waters) using an Aminex HDP-87H column (Bio-Rad) along with a Chrompak UV detector (detection at 210 nm) with 0.016 M H_2SO_4 as the eluent, running at 0.6 ml/min.

Alternatively, phenol, tyrosine, phenylalanine, and 4-hydroxyphenylpyruvate concentrations were determined simultaneously by HPLC (Agilent 1100 system) using a Zorbax 3.5-μm SB C_{18} column (length, 5 cm; inside diameter, 4.6 mm; particle size, 3.5 μm) with acetonitrile-KH_2PO_4 (0.05 M, pH 2, 1% acetonitrile) as the eluent. This setup allows for simultaneous detection at multiple wavelengths and online determination of UV/visible spectra.

RESULTS

Transcriptome analysis of phenol-producing *P. putida* S12TPL3 and sequencing of key genes. *P. putida* strain S12TPL3 was optimized for phenol production mostly by methods involving random mutagenesis. Comparative transcriptomics was applied in order to gain insight into the genetic changes in *P. putida* S12TPL3 connected to enhanced phenol production. To this end, both *P. putida* S12JNNmcs(t) and *P. putida* S12TPL3 (Table 1) were cultivated in chemostats. *P. putida* S12TPL3 produced approximately 500 μM phenol under these steady-state conditions. Phenol was added to this concentration to the feed of *P. putida* S12JNNmcs(t) to ensure equal growth conditions.

Transcriptome analysis yielded a total of 236 genes that showed at least a 1.8-fold change of the expression level in *P. putida* S12TPL3 compared to *P. putida* S12JNNmcs(t). Many of these genes encode hypothetical proteins and proteins with only a general function prediction. Other genes encode proteins previously shown to be related to solvent stress, such as alginate biosynthesis proteins (21); fatty acid metabolism proteins (38, 44); and antioxidants, chaperones, and heat shock proteins (10, 45). Genes involved in gluconate production and uptake (*gnuK* and *gntP*) were upregulated, likely as a result of the knockout of *oprB-1* in *P. putida* S12TPL3. The expression levels of other genes in the peripheral pathways of glucose metabolism (9) remained unchanged. The present study focuses on a group of 38 genes that were expected to have a more apparent link to phenol production.

The selected genes were grouped into five functional categories: tyrosine biosynthesis, tryptophan biosynthesis, aromatic degradation, amino acid transport, and the tricarboxylic acid (TCA) cycle (Table 2). The transcriptomes of strains *P. putida* S12TPL and *P. putida* S12TPL2 (Fig. 1) were analyzed in a similar manner, and the same trends in expression level were observed as in *P. putida* S12JNNmcs(t) and *P. putida* S12TPL3.

Since *N*-methyl-*N*′-nitro-*N*-nitrosoguanidine mutagenesis was used to obtain *P. putida* S12TPL3, point mutations that affect gene function were also expected to occur. As such mutations will not be detected with microarrays, the nucleotide sequences of several key genes related to tyrosine biosynthesis were determined in addition to the transcriptome analyses. The nucleotide sequences of three genes had changed in *P. putida* S12TPL3. The *aroF-2* gene, encoding a 3-deoxy-D-arabino-2-heptulosonic acid 7-phosphate (DAHP) synthase (PP3080), contained a point mutation resulting in a G136E substitution. The *trpE* gene, encoding anthranilate synthase component I (PP0417), contained a point mutation resulting in a P290S substitution. The *pykA* gene, encoding pyruvate kinase II (PP1362), contained a point mutation resulting in a V219A substitution. No mutations were found in the *tpl* gene and genes with KT2440 genome locus tags PP1866, PP2324 (*aroF-1*), PP0074 (*aroE-1*), PP3002 (*aroE-2*), PP1769 (*pheA*), PP2170, PP1770, PP4490 (*phhA*), PP1972 (*tyrB-1*), PP3590 (*tyrB-2*), and PP4621 (*hmgA*).

Expression profiles of genes in selected functional groups. (i) Tyrosine biosynthesis. Since phenol production from glucose proceeds via tyrosine in *P. putida* S12TPL3, major changes in the tyrosine biosynthetic pathway were expected (Fig. 2). Indeed, eight genes encoding enzymes involved in the biosynthesis of tyrosine were upregulated in *P. putida* S12TPL3. Six of these genes encode (*iso*-)enzymes in the early shikimate pathway, which is responsible for the conversion of phosphoenolpyruvate and erythrose-4-phosphate into shikimate. Two genes (*phhAB*) encode enzymes responsible for the conversion of phenylalanine into tyrosine.

(ii) Tryptophan biosynthesis. Tryptophan is produced from chorismate, which is also a precursor for tyrosine (Fig. 2) and thus for phenol in *P. putida* S12TPL3. The *trpE* gene and the *trpCDG* operon, required for the biosynthesis of tryptophan, are upregulated in *P. putida* S12TPL3. These genes are coregulated in *P. putida* (22).

(iii) Aromatic catabolism. Several pathways for degradation of intermediates of the tyrosine biosynthetic pathway exist in *P. putida* (17). The *pcaGH* genes (16); the *pcaCD*, *pcaF*, and *pcaIJ* genes (36); and the *pobA* gene (3) were upregulated in *P. putida* S12TPL3. These genes encode eight of the nine genes

TABLE 2. Genes with an apparent link to phenol production that are differentially expressed in *P. putida* S12TPL3 compared to control strain *P. putida* S12JNNmcs(t)

Functional group	Protein description (gene)	KT2440 locus tag	Fold change[a]
Tyrosine biosynthesis	DAHP synthase, class I (*aroF-1*)	PP2324	2.2
	Shikimate 5-dehydrogenase/quinate 5-dehydrogenase family protein	PP2406	2.7[b]
	3-Dehydroquinate dehydratase, type II	PP2407	6.3[b]
	Shikimate dehydrogenase family protein	PP2608	5.1[b]
	DAHP synthase, class I (*aroF-2*)	PP3080	21.1
	Quinate dehydrogenase (pyrroloquinoline quinone dependent), putative	PP3569	7.8
	Phenylalanine-4-hydroxylase (*phhA*)	PP4490	87.6
	Pterin-4-alpha-carbinolamine dehydratase (*phhB*)	PP4491	57.0
Tryptophan biosynthesis	Anthranilate synthase, component I (*trpE*)	PP0417	8.6
	Anthranilate synthase, component II (*trpG*)	PP0420	6.8
	Anthranilate phosphoribosyltransferase (*trpD*)	PP0421	6.3
	Indole-3-glycerol phosphate synthase (*trpC*)	PP0422	5.9
Aromatic degradation	4-Hydroxybenzoate transporter (*pcaK*)	PP1376	3.4[b]
	Beta-ketoadipyl coenzyme A thiolase (*pcaF*)	PP1377	7.1[b]
	3-Oxoadipate enol-lactone hydrolase (*pcaD*)	PP1380	2.1[b]
	4-Carboxymuconolactone decarboxylase (*pcaC*)	PP1381	1.9
	BenF-like protein	PP1383	25.1
	Tyrosine decarboxylase, putative	PP2552	3.7
	4-Hydroxyphenylpyruvate dioxygenase, putative	PP2554	3.8[b]
	Fumarylacetoacetate hydrolase family protein	PP2836	29.3
	4-Hydroxyphenylpyruvate dioxygenase (*hpd*)	PP3433	2.8
	4-Hydroxybenzoate hydroxylase (*pobA*)	PP3537	2.4[b]
	3-Oxoadipate coenzyme A transferase, subunit A (*pcaI*)	PP3951	5.0[b]
	3-Oxoadipate coenzyme A transferase, subunit B (*pcaJ*)	PP3952	3.2
	Protocatechuate 3,4-dioxygenase, alpha subunit (*pcaG*)	PP4655	2.9
	Protocatechuate 3,4-dioxygenase, beta subunit (*pcaH*)	PP4656	4.9[b]
Amino acid transport	Transporter, LysE family	PP0198	2.1
	Branched-chain amino acid ABC transporter, ATP-binding protein	PP0615	0.6
	Branched-chain amino acid ABC transporter, permease protein	PP0618	0.4
	Branched-chain amino acid ABC transporter, periplasmic amino acid-binding protein	PP0619	0.5
	Aromatic amino acid transporter (*aroP2*)	PP0927	10.7
	Amino acid ABC transporter, permease protein	PP1070	0.5
	Amino acid efflux protein, putative	PP3023	2.1
	Aromatic amino acid transporter (*aroP1*)	PP4495	10.5
TCA cycle	Fumarate hydratase, class I	PP0897	0.5
	Oxidoreductase, Ldh family	PP2835	111.5
	Isocitrate dehydrogenase, NADP dependent, prokaryotic type	PP4011	1.9
	Malic enzyme	PP5085	2.2

[a] Fold change in expression level in *P. putida* S12TPL3 compared to *P. putida* S12JNNmcs(t).
[b] There was a large variation of expression levels between duplicates of *P. putida* S12TPL3. The average fold changes shown were confirmed by RT-qPCR.

necessary for the degradation of 4-hydroxybenzoate via the protocatechuate degradation pathway. This pathway can be linked to the tyrosine biosynthetic pathway through a chorismate-pyruvate lyase (PP5317) that converts chorismate into 4-hydroxybenzoate (Fig. 2). This link was confirmed by our observation that a *pobA hpd* double knockout mutant produced 4-hydroxybenzoate and showed, as a result of these mutations, a significantly decreased growth yield when cultured on quinate as a sole carbon source. Quinate can be metabolized only by conversion into chorismate, as was illustrated by the inability of an *aroK* (shikimate kinase) knockout mutant to utilize quinate as a carbon source (unpublished data).

The *hpd* gene and two genes with locus tags PP2554 and PP2836 were upregulated in *P. putida* S12TPL3. These genes encode enzymes in the homogentisate degradation pathway (1). Tyrosine can be degraded via this pathway, with 4-hydroxyphenylpyruvate as an intermediate.

(iv) Amino acid transport. A wide range of transport systems for amino acids were found to be differentially expressed in *P. putida* S12TPL3. Several genes encoding proteins capable of amino acid export were upregulated, including two *aroP* genes for aromatic amino acid transporters and a LysE family transporter. Conversely, systems for the uptake of amino acids, such as the branched-chain amino acid ABC transporter, were downregulated.

(v) TCA cycle. Four genes encoding enzymes in the TCA cycle were found to be differentially expressed in *P. putida* S12TPL3. Of these genes, three were upregulated.

Verification of leads from the transcriptome analysis. Based on the transcriptome analysis, four genes that were upregulated in *P. putida* S12TPL3 were selected as targets for disrup-

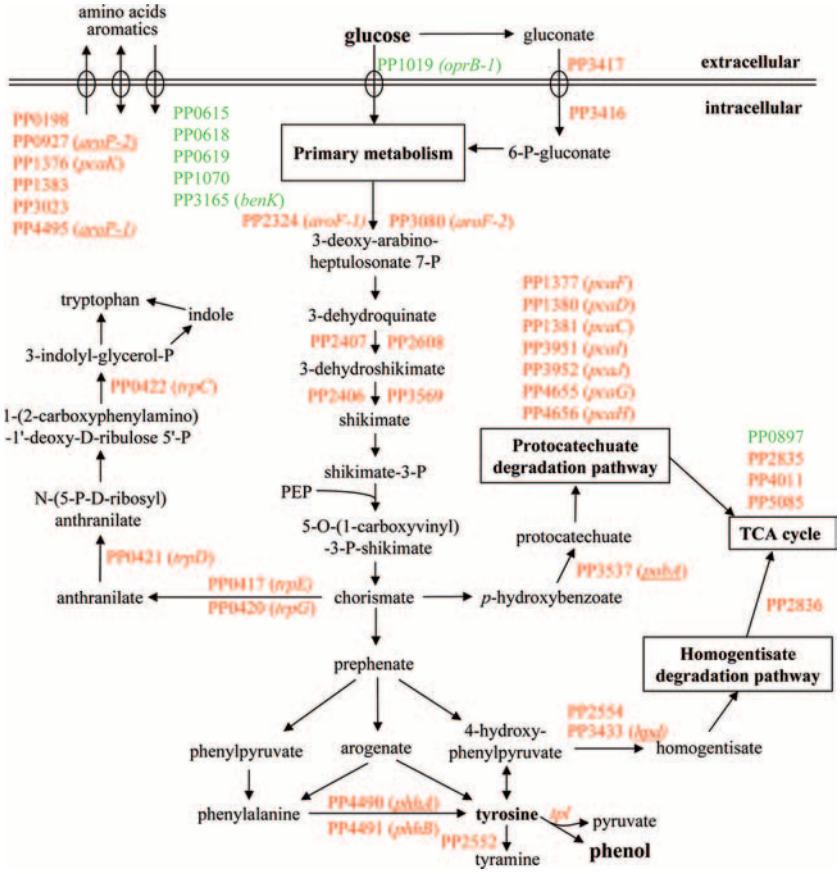

FIG. 2. Schematic overview of expression profiles of genes involved in relevant pathways of phenol production, as derived from transcriptome analysis of *P. putida* S12TPL3. Genes are indicated by locus tags from *P. putida* KT2440, followed by their gene name in parentheses where applicable. Green lettering indicates downregulation, and red indicates upregulation. Genes that were selected for targeted disruption are underlined.

tion in *P. putida* S12TPL3 (Fig. 2) in order to gain further insight into the enhanced phenol production characteristics of this strain. The *hpd* and *pobA* genes (locus tags PP3433 and PP3537, respectively) are responsible for degradation of shikimate pathway products. Disruption of these genes was expected to decrease the degradation of shikimate pathway intermediates, resulting in increased tyrosine production. The *phhA* gene (PP4490) is responsible for the conversion of phenylalanine into tyrosine. Disruption of this gene will give insight into what portion of the tyrosine is produced via phenylalanine, rather than directly via 4-hydroxyphenylpyruvate (Fig. 2). The *aroP1* gene (PP4495) is responsible for transport of aromatic amino acids. Disruption of this gene could decrease export of tyrosine, increasing the intracellular tyrosine pool available to the TPL enzyme for phenol production.

The selected genes were disrupted in *P. putida* S12TPL3. As a control strain, *P. putida* S12TPL3r (Table 1) was used. As expected, *P. putida* STΔphhA showed deteriorated production characteristics (Fig. 3D). The other mutants showed a decreased phenol productivity compared to *P. putida* S12TPL3 as well, although not as drastic as in strain STΔphhA. Unexpectedly, *P. putida* S12TPL3r also showed a decreased phenol productivity, comparable to that of the *hpd* and *pobA* knockout mutants (Fig. 3). This observation suggested that the curing and retransformation procedure intrinsically affected phenol production. The *aroP1* knockout mutant showed impaired growth and also produced slightly less phenol than strain S12TPL3r (data not shown). A mutant with a double knockout of both isogenes *aroP1* and *aroP2* did not grow at all on minimal glucose medium.

All strains continued to produce phenol after growth had ceased (Fig. 3); however, the delay in production was more pronounced for the knockout strains and the retransformed control strain than for strain S12TPL3. The effect was most distinct in *P. putida* STΔhpd: as much as 62% of the phenol was produced after growth, compared to 28% in *P. putida* S12TPL3. Therefore, we speculated that an intermediate of the late tyrosine biosynthetic pathway accumulated, which was later converted into phenol. HPLC analyses of culture supernatant samples indeed indicated the presence of an aromatic compound with the same retention time and UV spectrum as 4-hydroxyphenylpyruvate. Since 4-hydroxyphenylpyruvate is unstable under the conditions used, exact determination of the concentration was not possible. One of the chemical degradation products overlaps with the 4-hydroxyphenylpyruvate peak. Therefore, the sum of the overlapping peak areas of 4-hydroxyphenylpyruvate and the degradation product was used to estimate the concentration of 4-hydroxyphenylpyruvate as accu-

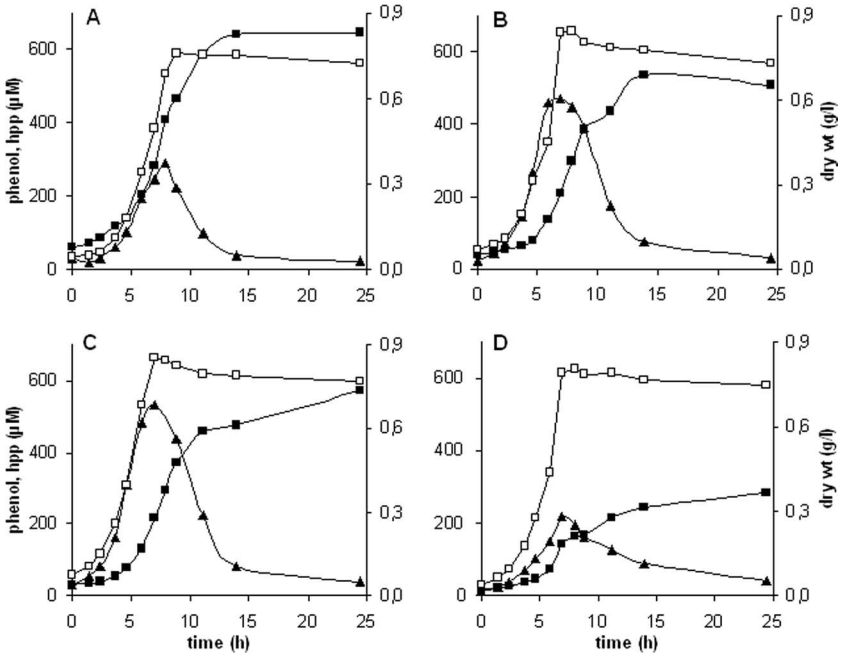

FIG. 3. Production and growth of *P. putida* S12TPL3 (A), *P. putida* S12TPL3r (B), *P. putida* STΔhpd (C), and *P. putida* STΔphhA (D). □, cell dry weight; ■, phenol concentration; ▲, estimated 4-hydroxyphenylpyruvate (hpp) concentration. The profiles for strains STΔpobA and STΔhpd were similar; therefore, only results for STΔhpd are presented here. Cultures were performed in triplicate in mineral salts medium with 10 mM glucose as the carbon source. The variation between replicates was less than 10%.

rately as possible (Fig. 3). Tyrosine and phenylalanine were also found, albeit in trace quantities.

Identification of bottlenecks for phenol production in *P. putida* S12TPL3. The mutants that were expected to have an increased carbon flux toward tyrosine (Δ*pobA* and Δ*hpd* mutants) did not show an increase in phenol production. The secretion of 4-hydroxyphenylpyruvate, a direct precursor of tyrosine, suggests that the bottleneck is either the conversion of 4-hydroxyphenylpyruvate into tyrosine or the conversion of tyrosine into phenol, causing the pathway to overflow to 4-hydroxyphenylpyruvate. Thus, we investigated whether TPL activity or tyrosine availability was the limiting factor for phenol production in *P. putida* S12TPL3. To study the effect of tyrosine availability, *P. putida* S12TPL3 was cultivated in a chemostat on mineral salts medium with 10 mM glucose as the growth-limiting nutrient. Phenol production was assessed either after addition of a tyrosine pulse or with a continuous feed of tyrosine.

For the pulse experiment, L-tyrosine was added to a steady-state culture to a final concentration of 845 μM. The phenol, tyrosine, and 4-hydroxyphenylpyruvate concentrations were monitored (Fig. 4). After 160 min, the phenol concentration in the culture had increased from 456 μM at steady state to a maximum of 560 μM. At the same time, the 4-hydroxyphenylpyruvate concentration had increased from 44 μM before the pulse to 232 μM after 160 min. The amount of biomass in the fermentor during this time remained constant at 0.59 g (dry weight) liter^{-1}. The phenol production rate of the culture had increased 1.2-fold, from 4.8 to 5.9 μmol (g protein)$^{-1}$ min^{-1}, while the 4-hydroxyphenylpyruvate production rate increased almost fivefold from 0.5 to 2.4 μmol (g protein)$^{-1}$ min^{-1}. The average tyrosine uptake rate was 7.0 μmol (g protein)$^{-1}$ min^{-1}. The uptake of tyrosine did not result in an equivalent increase in phenol production. Most of the tyrosine was converted into 4-hydroxyphenylpyruvate instead.

In order to mimic increased biosynthesis of tyrosine in the cells, L-tyrosine (1 mM) was added to the influent of the chemostat culture, and after reaching steady state, the phenol concentration was measured. With tyrosine in the influent, 611 μM phenol was produced, compared to 456 μM without tyrosine in the influent. The biomass had increased to 0.75 g (dry weight) liter^{-1}. The specific production rate of phenol in-

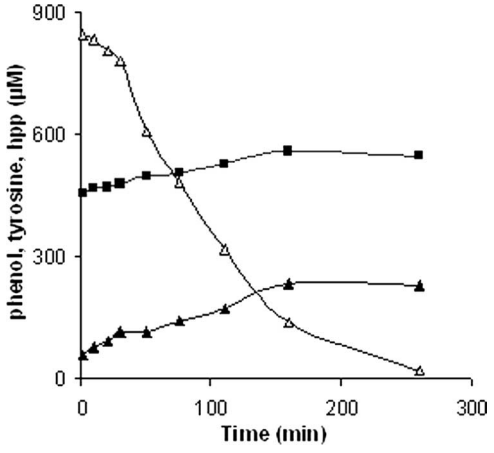

FIG. 4. Phenol and 4-hydroxyphenylpyruvate production in chemostat cultures of *P. putida* S12TPL3 after a tyrosine pulse. ■, phenol concentration; △, tyrosine concentration; ▲, estimated 4-hydroxyphenylpyruvate (hpp) concentration. Values are the averages from duplicate experiments; variation between duplicates was less than 10%.

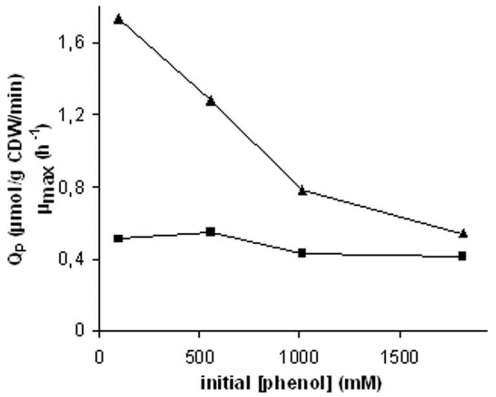

FIG. 5. Phenol production by *P. putida* S12TPL3 in mineral salts medium with 20 mM glucose as the carbon source in the presence of different concentrations of phenol in the culture medium. ■, maximum growth rate (h^{-1}); ▲, Q_p (average specific activity during the first 12 h of cultivation) [μmol (g cell dry weight)$^{-1}$ min^{-1}].

creased only marginally, from 4.9 to 5.0 μmol (g protein)$^{-1}$ min^{-1}. Thus, the increased phenol accumulation can be explained by the increased biomass density brought about by the utilization of tyrosine as an additional carbon source.

These results show that only a small amount of the additional tyrosine in the cell is converted into phenol under the conditions applied. Most tyrosine was converted into biomass, via 4-hydroxyphenylpyruvate. This suggests that TPL activity is the limiting factor for phenol production in *P. putida* S12TPL3, rather than tyrosine availability.

TPL activity in *P. putida* cell extracts and effect of exogenously added phenol on phenol production. Since TPL appears to be the limiting factor for phenol production, TPL activity in cell extracts of *P. putida* S12TPL3 in the presence and absence of phenol was investigated. The specific TPL activity was greatly affected by the presence of phenol. In the presence of 1 mM of phenol, only 23% of the original activity remained [23.2 μmol (g protein)$^{-1}$ min^{-1} without phenol and 5.3 μmol (g protein)$^{-1}$ min^{-1} with 1 mM phenol]. Thus, it may be expected that the presence of phenol seriously affects its own production, through the inhibition of TPL (19, 28). This was confirmed by testing the phenol production of *P. putida* S12TPL3 grown in shake flask cultures in the presence of different concentrations of exogenously added phenol (Fig. 5). The effect of phenol on the μ_{max} of the cultures was relatively small, but a drastic negative effect on phenol production was observed.

TPL activity in cell extract of *P. putida* STΔhpd was also compared to that in *P. putida* S12TPL3. Cells of both strains were harvested in logarithmic phase to ensure optimal comparability. The maximum specific activity of TPL in extracts of *P. putida* STΔhpd was 2.2 μmol (g protein)$^{-1}$ min^{-1}, which is about 30% of the activity in *P. putida* S12TPL3 [7.8 μmol (g protein)$^{-1}$ min^{-1}]. This decreased TPL activity is likely to explain the decreased phenol production and the increased 4-hydroxyphenylpyruvate production in this mutant. As the TPL expression plasmid used to transform the knockout mutants was isolated from strain S12TPL3, differences in the expression plasmid are excluded. Furthermore, no mutations in the *tpl* gene were observed in this plasmid (data not shown). Possibly, the lowered TPL activity may be explained by a copy number effect. The same effect may be expected for the other strains that were cured and retransformed with plasmid pNW1C, i.e., the retransformed parent strain (S12TPL3r) and the other knockout mutants.

DISCUSSION

The approach that yielded the optimized phenol producer *P. putida* S12TPL3 entailed several steps based on random procedures (49). In the present study, the effects on the cellular events associated with this enhanced phenol production were investigated by chemostat-based comparative transcriptomics, complemented with nucleotide sequencing of key genes. The observed altered transcription profiles in *P. putida* S12TPL3 could be linked to (i) cellular events effectuating improved metabolic flux toward L-tyrosine and hence toward phenol and (ii) events responding to this improved flux.

The upregulated genes of the tyrosine biosynthetic pathway fall into the first category. Almost all upregulated genes encoded enzymes in the early shikimate pathway, i.e., the first steps of aromatic amino acid biosynthesis. Of the sequenced early pathway genes, only *aroF-2* contained a mutation, which was expected to have little effect, as the resulting amino acid substitution (G136E) also occurs in orthologues of *Pseudomonas fluorescens* strains (5). An increased metabolic flux through the early shikimate pathway, as indicated by the transcriptome data for strain S12TPL3, caused more carbon to flow toward phenylalanine in *Pseudomonas aeruginosa* (11). Tyrosine was produced from phenylalanine via an "overflow pathway" encoded by the *phhAB* genes, which are induced by phenylalanine (15). Our findings that the *phhAB* genes were highly upregulated in *P. putida* S12TPL3 and that disruption of *phhA* decreased phenol production by 60% were in agreement with these results. The upregulation of four genes involved in tryptophan biosynthesis (*trpCDGE*) suggests that the intracellular tryptophan pool was decreased in *P. putida* S12TPL3 (22). This decrease can be attributed to a mutation in the *trpE* gene, resulting in a P290S substitution adjacent to the catalytic site of the encoded anthranilate synthase component I (42). A decreased tryptophan pool contributes to the enhanced phenol production at two levels: less carbon will be directed into the tryptophan branch of the shikimate pathway, and the tryptophan-inhibited DAHP synthase could more effectively contribute to the overall carbon flux into the shikimate pathway. Thus, the transcriptome analyses indicate that the increased carbon flux toward tyrosine and, thus, phenol in strain S12TPL3 may be attributed to an upregulated early shikimate pathway, combined with a decreased carbon flux through the tryptophan branch.

The observed upregulation of genes involved in aromatic degradation pathways (1, 17), such as the homogentisate and the protocatechuate pathways, can be categorized in the second group of transcriptional events. The upregulation of these genes indicate high intracellular levels of tyrosine or its intermediates. This suggested that in *P. putida* S12TPL3, tyrosine is synthesized faster than it is converted into phenol. This would imply that TPL is the bottleneck in phenol synthesis. A strong indication that this is the case in *P. putida* S12TPL3 was provided by the tyrosine pulse and feed experiments that demon-

strated that surplus tyrosine was converted mostly into 4-hydroxyphenylpyruvate (and eventually biomass) rather than into phenol. More indications that TPL limited phenol production was provided by the targeted knockout mutants of the first genes of the homogentisate and protocatechuate pathways (*hpd* and *pobA*). Also in these strains, increased 4-hydroxyphenylpyruvate levels rather than increased phenol levels were observed, indicating carbon overflow from accumulated tyrosine and showing that TPL was the limiting factor.

Other responses that indicated higher intracellular levels of tyrosine and/or its precursors were the upregulation of at least some of the putative amino acid transporters and the upregulation of three genes encoding TCA cycle enzymes. The most prominent amino acid transporters were the two *aroP* isogenes, each of which showed over 10-fold-higher expression levels. AroP-type transporters regulate intracellular pools of aromatic amino acids by balancing import and export (4). The *aroP* genes appear to be important in *P. putida* S12TPL3, since an *aroP1 aroP2* double knockout mutant did not grow at all on minimal glucose medium (unpublished data), and an *aroP1* single knockout mutant showed decreased phenol production. As the tyrosine precursor 4-hyroxyphenylpyruvate rather than tyrosine itself accumulated in strain S12TPL3, it may be speculated that AroP1 and AroP2 act as metabolic relief valves for this tyrosine precursor. The possibility of AroP1 and AroP2 as phenol transporters can be excluded, since the double knockout mutant does not grow on mineral medium in the absence of the *tpl* expression vector either. The induction of TCA cycle genes may be linked to the accumulation of phenol. Such a response has previously been observed in solvent-stressed pseudomonads, as a means to increase the energy supply required by the solvent tolerance response (41, 45). The upregulation of the malic enzyme may be attributed to the surplus production of pyruvate from tyrosine by TPL (26).

In conclusion, transcriptome and nucleotide sequence analyses have provided profound and novel insights into the genetic basis of the enhanced phenol production by *P. putida* S12TPL3, as well as in the cellular responses brought about by the enhanced metabolic flux toward tyrosine and the production of phenol. In strain S12TPL3, the carbon flow toward tyrosine was optimized to such an extent that TPL activity had become the bottleneck for phenol production. Based on these detailed insights, a rational approach for further optimization of phenol production can be pursued, with a primary focus on enhancement of TPL activity.

ACKNOWLEDGMENTS

We thank Maaike Westerhof for her assistance with the targeted gene disruptions. We also thank Suzanne Verhoef for providing strain *P. putida* STΔpobA and the *pobA hpd* double knockout mutant and Nicole van Luijk for providing the *aroP1 aroP2* double knockout mutant of *P. putida* S12TPL3.

REFERENCES

1. **Arias-Barrau, E., E. R. Olivera, J. M. Luengo, C. Fernandez, B. Galan, J. L. Garcia, E. Diaz, and B. Minambres.** 2004. The homogentisate pathway: a central catabolic pathway involved in the degradation of L-phenylalanine, L-tyrosine, and 3-hydroxyphenylacetate in *Pseudomonas putida*. J. Bacteriol. **186:**5062–5077.
2. **Ballerstedt, H., R. J. M. Volkers, A. E. Mars, J. E. Hallsworth, V. A. Martins dos Santos, J. Puchalka, J. Duuren, G. Eggink, K. N. Timmis, J. A. M. de Bont, and J. Wery.** 2007. Genomotyping of *Pseudomonas putida* strains using *P. putida* KT2440-based high-density DNA microarrays: implications for transcriptomics studies. Appl. Microbiol. Biotechnol. **75:**1133–1142.
3. **Bertani, I., M. Kojic, and V. Venturi.** 2001. Regulation of the p-hydroxybenzoic acid hydroxylase gene (*pobA*) in plant-growth-promoting *Pseudomonas putida* WCS358. Microbiology **147:**1611–1620.
4. **Brown, K. D.** 1971. Maintenace and exchange of the aromatic amino acid pool in *Escherichia coli*. J. Bacteriol. **106:**70–81.
5. **Byng, G. S., A. Berry, and R. A. Jensen.** 1983. A pair of regulatory isozymes for 3-deoxy-D-arabino-heptulosonate 7-phosphate synthase is conserved within group I pseudomonads. J. Bacteriol. **156:**429–433.
6. **Choi, J. H., S. J. Lee, and S. Y. Lee.** 2003. Enhanced production of insulin-like growth factor I fusion protein in *Escherichia coli* by coexpression of the down-regulated genes identified by transcriptome profiling. Appl. Environ. Microbiol. **69:**4737–4742.
7. **de Bont, J. A. M.** 1998. Solvent-tolerant bacteria in biocatalysis. Tibtech **16:**493–499.
8. **Dejonghe, W., N. Boon, D. Seghers, E. M. Top, and W. Verstraete.** 2001. Bioaugmentation of soils by increasing microbial richness: missing links. Environ. Microbiol. **3:**649–657.
9. **del Castillo, T., J. L. Ramos, J. J. Rodriguez-Herva, T. Fuhrer, U. Sauer, and E. Duque.** 2007. Convergent peripheral pathways catalyze initial glucose catabolism in *Pseudomonas putida*: genomic and flux analysis. J. Bacteriol. **189:**5142–5152.
10. **Dominguez-Cuevas, P., J. E. Gonzalez-Pastor, S. Marques, J. L. Ramos, and V. de Lorenzo.** 2006. Transcriptional tradeoff between metabolic and stress-response programs in *Pseudomonas putida* KT2440 cells exposed to toluene. J. Biol. Chem. **281:**11981–11991.
11. **Fiske, M. J., R. J. Whitaker, and R. A. Jensen.** 1983. Hidden overflow pathway to L-phenylalanine in *Pseudomonas aeruginosa*. J. Bacteriol. **154:**623–631.
12. **Godard, P., A. Urrestarazu, S. Vissers, K. Kontos, G. Bontempi, J. van Helden, and B. Andre.** 2007. Effect of 21 different nitrogen sources on global gene expression in the yeast *Saccharomyces cerevisiae*. Mol. Cell. Biol. **27:**3065–3086.
13. **Hartmans, S., J. P. Smits, M. J. van der Werf, F. Volkering, and J. A. M. de Bont.** 1989. Metabolism of styrene oxide and 2-phenyl ethanol in the styrene degrading *Xanthobacter* strain 124X. Appl. Environ. Microbiol. **55:**2850–2855.
14. **Hayashi, S., R. Aono, T. Hanai, H. Mori, T. Kobayashi, and H. Honda.** 2003. Analysis of organic solvent tolerance in *Escherichia coli* using gene expression profiles from DNA microarrays. J. Biosci. Bioeng. **95:**379–383.
15. **Herrera, M. C., and J. L. Ramos.** 2007. Catabolism of phenylalanine by *Pseudomonas putida*: the NtrC-family PhhR regulator binds to two sites upstream from the phhA gene. J. Mol. Biol. **366:**1374–1386.
16. **Hosokawa, K.** 1970. Regulation of synthesis of early enzymes of p-hydroxybenzoate pathway in *Pseudomonas putida*. J. Biol. Chem. **245:**5304–5308.
17. **Jimenez, J. I., B. Minambres, J. L. Garcia, and E. Diaz.** 2002. Genomic analysis of the aromatic catabolic pathways from *Pseudomonas putida* KT2440. Environ. Microbiol. **4:**824–841.
18. **Kieboom, J., J. J. Dennis, J. A. M. de Bont, and G. J. Zylstra.** 1998. Identification and molecular characterization of an efflux pump involved in *Pseudomonas putida* S12 solvent tolerance. J. Biol. Chem. **273:**85–91.
19. **Kumagai, H., and H. Yamada.** 1970. Tyrosine phenol lyase. I. Purification, crystallization and properties. J. Biol. Chem. **245:**1767–1772.
20. **Lee, J. H., D. E. Lee, B. U. Lee, and H. S. Kim.** 2003. Global analyses of transcriptomes and proteomes of a parent strain and an L-threonine-overproducing mutant strain. J. Bacteriol. **185:**5442–5451.
21. **Leone, S., A. Molinaro, F. Alfieri, V. Cafaro, R. Lanzetta, A. Di Donato, and M. Parrilli.** 2006. The biofilm matrix of *Pseudomonas* sp. OX1 grown on phenol is mainly constituted by alginate oligosaccharides. Carbohydr. Res. **341:**2456–2461.
22. **Maurer, R., and I. P. Crawford.** 1971. New regulatory mutation affecting some of the tryptophan genes in *Pseudomonas putida*. J. Bacteriol. **106:**331–338.
23. **Nelson, K. E., C. Weinel, I. T. Paulsen, R. J. Dodson, H. Hilbert, V. A. Martins dos Santos, D. E. Fouts, S. R. Gill, M. Pop, M. Holmes, L. Brinkac, M. Beanan, R. T. DeBoy, S. Daugherty, J. Kolonay, R. Madupu, W. Nelson, O. White, J. Peterson, H. Khouri, I. Hance, P. Chris Lee, E. Holtzapple, D. Scanlan, K. Tran, A. Moazzez, T. Utterback, M. Rizzo, K. Lee, D. Kosack, D. Moestl, H. Wedler, J. Lauber, D. Stjepandic, J. Hoheisel, M. Straetz, S. Heim, C. Kiewitz, J. A. Eisen, K. N. Timmis, A. Dusterhoft, B. Tümmler, and C. M. Fraser.** 2002. Complete genome sequence and comparative analysis of the metabolically versatile *Pseudomonas putida* KT2440. Environ. Microbiol. **4:**799–808.
24. **Nijkamp, K., N. van Luijk, J. A. M. de Bont, and J. Wery.** 2005. The solvent-tolerant *Pseudomonas putida* S12 as host for the production of cinnamic acid from glucose. Appl. Microbiol. Biotechnol. **69:**170–177.
25. **Park, J. H., K. H. Lee, T. Y. Kim, and S. Y. Lee.** 2007. Metabolic engineering of *Escherichia coli* for the production of L-valine based on transcriptome analysis and in silico gene knockout simulation. Proc. Natl. Acad. Sci. USA **104:**7797–7802.
26. **Park, S. J., P. A. Cotter, and R. P. Gunsalus.** 1995. Regulation of malate dehydrogenase (*mdh*) gene expression in *Escherichia coli* in response to oxygen, carbon, and heme availability. J. Bacteriol. **177:**6652–6656.

27. **Park, S. J., S. Y. Lee, J. Cho, T. Y. Kim, J. W. Lee, J. H. Park, and M. J. Han.** 2005. Global physiological understanding and metabolic engineering of microorganisms based on omics studies. Appl. Microbiol. Biotechnol. **68:**567–579.
28. **Pletnev, S. V., M. N. Isupov, Z. Dauter, K. S. Wilson, N. G. Faleev, E. G. Harutyunyan, and T. V. Demidkina.** 1996. Purification and crystals of tyrosine phenol-lyase from *Erwinia herbicola*. Biochem. Mol. Biol. Int. **38:**37–42.
29. **Polen, T., M. Kramer, J. Bongaerts, M. Wubbolts, and V. F. Wendisch.** 2005. The global gene expression response of *Escherichia coli* to L-phenylalanine. J. Biotechnol. **115:**221–237.
30. **Quandt, J., and M. F. Hynes.** 1993. Versatile suicide vectors which allow direct selection for gene replacement in Gram-negative bacteria. Gene **127:** 15–21.
31. **Ramos, J. L., E. Duque, M. T. Gallegos, P. Godoy, M. I. Ramos-Gonzalez, A. Rojas, W. Teran, and A. Segura.** 2002. Mechanisms of solvent tolerance in gram-negative bacteria. Annu. Rev. Microbiol. **56:**743–768.
32. **Ramos, J. L., E. Duque, J. J. Rodriguez-Herva, P. Godoy, A. Haidour, F. Reyes, and A. Fernandez-Barrero.** 1997. Mechanisms for solvent tolerance in bacteria. J. Biol. Chem. **272:**3887–3890.
33. **Ramos-Gonzalez, M. I., A. Ben-Basat, M. J. Campos, and J. L. Ramos.** 2003. Genetic engineering of a highly solvent-tolerant *Pseudomonas putida* strain for biotransformation of toluene to *p*-hydroxybenzoate. Appl. Environ. Microbiol. **69:**5120–5127.
34. **Reva, O. N., C. Weinel, M. Weinel, K. Bohm, D. Stjepandic, J. D. Hoheisel, and B. Tümmler.** 2006. Functional genomics of stress response in *Pseudomonas putida* KT2440. J. Bacteriol. **188:**4079–4092.
35. **Rojas, A., E. Duque, A. Schmid, A. Hurtado, J. L. Ramos, and A. Segura.** 2004. Biotransformation in double-phase systems: physiological responses of *Pseudomonas putida* DOT-T1E to a double phase made of aliphatic alcohols and biosynthesis of substituted catechols. Appl. Environ. Microbiol. **70:**3637–3643.
36. **Romero-Steiner, S., R. E. Parales, C. S. Harwood, and J. E. Houghton.** 1994. Characterization of the *pcaR* regulatory gene from *Pseudomonas putida*, which is required for the complete degradation of *p*-hydroxybenzoate. J. Bacteriol. **176:**5771–5779.
37. **Sambrook, J., E. F. Fritsch, and T. Maniatis.** 1982. Molecular cloning: a laboratory manual, 2nd ed. Cold Spring Harbor Laboratory Press, Cold Spring Harbor, NY.
38. **Santos, P. M., D. Benndorf, and I. Sa-Correia.** 2004. Insights into *Pseudomonas putida* KT2440 response to phenol-induced stress by quantitative proteomics. Proteomics **4:**2640–2652.
39. **Sardessai, Y. N., and S. Bhosle.** 2004. Industrial potential of organic solvent tolerant bacteria. Biotechnol. Prog. **20:**655–660.
40. **Schmid, A., J. S. Dordick, B. Hauer, A. Kiener, M. Wubbolts, and B. Witholt.** 2001. Industrial biocatalysis today and tomorrow. Nature **409:**258–268.
41. **Segura, A., P. Godoy, P. van Dillewijn, A. Hurtado, N. Arroyo, S. Santacruz, and J. L. Ramos.** 2005. Proteomic analysis reveals the participation of energy- and stress-related proteins in the response of *Pseudomonas putida* DOT-T1E to toluene. J. Bacteriol. **187:**5937–5945.
42. **Spraggon, G., C. Kim, X. Nguyen-Huu, M. C. Yee, C. Yanofsky, and S. E. Mills.** 2001. The structures of anthranilate synthase of *Serratia marcescens* crystallized in the presence of (i) its substrates, chorismate and glutamine, and a product, glutamate, and (ii) its end-product inhibitor, L-tryptophan. Proc. Natl. Acad. Sci. USA **98:**6021–6026.
43. **Verhoef, S., H. J. Ruijssenaars, J. A. M. de Bont, and J. Wery.** 2007. Bioproduction of p-hydroxybenzoate from renewable feedstock by solvent-tolerant *Pseudomonas putida* S12. J. Biotechnol. **132:**49–56.
44. **Volker, U., and M. Hecker.** 2005. From genomics via proteomics to cellular physiology of the Gram-positive model organism *Bacillus subtilis*. Cell. Microbiol. **7:**1077–1085.
45. **Volkers, R. J. M., A. L. de Jong, A. G. Hulst, B. L. M. van Baar, J. A. M. de Bont, and J. Wery.** 2006. Chemostat-based proteomic analysis of toluene-affected *Pseudomonas putida* S12. Environ. Microbiol. **8:**1674–1679.
46. **Wackett, L. P.** 2003. *Pseudomonas putida*—a versatile biocatalyst. Nat. Biotechnol. **21:**136–138.
47. **Weber, F. J., L. P. Ooijkaas, R. M. Schemen, S. Hartmans, and J. A. M. de Bont.** 1993. Adaptation of *Pseudomonas putida* S12 to high concentrations of styrene and other organic solvents. Appl. Environ. Microbiol. **59:**3502–3504.
48. **Wery, J., and J. A. M. de Bont.** 2004. Solvent-tolerance of pseudomonads: a new degree of freedom in biocatalysis, p. 609–634. *In* J. L. Ramos (ed.), Pseudomonas, vol. 3. Kluwer Academic, Dordrecht, The Netherlands.
49. **Wery, J., B. Hidayat, J. Kieboom, and J. A. M. de Bont.** 2001. An insertion sequence prepares *Pseudomonas putida* S12 for severe solvent stress. J. Biol. Chem. **276:**5700–5706.
50. **Wery, J., D. I. Mendes da Silva, and J. A. M. de Bont.** 2000. A genetically modified solvent-tolerant bacterium for optimized production of a toxic fine chemical. Appl. Microbiol. Biotechnol. **54:**180–185.
51. **Wierckx, N. J. P., H. Ballerstedt, J. A. M. de Bont, and J. Wery.** 2005. Engineering of solvent-tolerant *Pseudomonas putida* S12 for bioproduction of phenol from glucose. Appl. Environ. Microbiol. **71:**8221–8227.